Molecular Orientation in Novolac Cured Epoxy Resins as Studied by Rheo-optical FTIR Spectroscopy

TOM SCHERZER

Institut für Oberflächenmodifizierung, Permoserstrasse 15, D-04318 Leipzig, Germany

Received 17 September 1997; accepted 5 March 1998

ABSTRACT: The molecular orientation and relaxation behavior was studied by rheooptical FTIR spectroscopy during the uniaxial deformation of epoxy resins prepared from the diglycidyl ether of butanediol and novolacs on the basis of bisphenol A. The investigation of orientation phenomena was performed in both the rubbery and the glassy state of the epoxies. Results are discussed with regard to the respective mechanism of deformation. Moreover, the effect of temperature, strain rate, and the molecular weight of the novolacs used on the orientation behavior and the mechanical properties was studied. A significant influence of these parameters on the molecular deformation behavior was observed. The reversibility of the orientation at temperatures above and below the glass transition temperature was examined. Epoxy films were subjected to successive loading–unloading cycles including elongation, relaxation, and annealing. The investigations show that the orientation is completely reversible in the rubbery state, but it is only partly reversible below the glass temperature. © 1998 John Wiley & Sons, Inc. J Appl Polym Sci 70: 247–259, 1998

Key words: novolac cured epoxy resins; rheooptical FTIR spectroscopy; molecular orientation and relaxation phenomena; temperature dependence of orientation behavior; reversibility of orientation; molecular mechanism of deformation

INTRODUCTION

Epoxy resins have found widespread use as engineering thermoset materials because of their high performance with respect to mechanical, thermal, and electrical properties; their chemical and environmental resistance; and their excellent adhesion to many materials. For many technical applications, the mechanical properties are of outstanding significance. The macroscopic mechanical behavior is strongly influenced not only by the morphological structure of the epoxies but also by their molecular deformation and orientation behavior. The characterization of such orientation effects on a molecular scale is crucial for the better understanding of the relationships between microscopic deformation behavior and mechanical properties. In particular, molecular orientation studies carried out simultaneously with mechanical treatment provide essential contributions to a more comprehensive knowledge about the complex mechanisms of polymer deformation.

Rheooptical FTIR spectroscopy is a powerful and versatile technique for monitoring transient structural changes during the deformation process. It offers a unique possibility to obtain detailed information about molecular orientation and relaxation behavior occurring during elongation, recovery, stress relaxation, and fatigue and to correlate it with macroscopic properties. A wide variety of polymers, including epoxy resins, have been studied by the means of rheooptical FTIR spectroscopy.[1–11] Previous articles[12–14] reported the results from the application of rheooptical FTIR spectroscopy to the characterization of ori-

Journal of Applied Polymer Science, Vol. 70, 247–259 (1998)
 CCC 0021-8995/98/020261-13

Table I Description of Novolacs on Basis of Bisphenol A

Novolac	DNL 7.5	DNL 15
Ratio of paraformaldehyde to bisphenol A (mol/mol)	0.57	1.13
Methylene bridges/mol bisphenol A (mol)	0.6	0.85
$\bar{M}_n$ (g/mol)	590	820
T_g (°C)	54.3	59.1

Data taken from Strehmel et al.[21]

entation phenomena in polyetheramine cured diglycidyl ether of bisphenol A (DGEBA) during uniaxial deformation.

Many epoxy resins are quite brittle materials. However, their toughness can be improved by the addition of various fillers to the resin mixture. On the other hand, the intrinsic toughness of the epoxy matrix itself can also be improved. The most common way to increase the intrinsic toughness of thermosets is the variation of the crosslink density.[15] Heterogeneities also have a large influence on the toughness.

In the present study, novolacs based on bisphenol A and paraformaldehyde were used as curing agents for an aliphatic epoxy resin. Epoxy novolacs and novolac cured epoxies are known to show much higher toughness than most other epoxy resins.[16–18] The high toughness of the novolac based systems is due to their heterogeneous network structure.[16,19,20]

Novolacs show a broad molecular weight distribution. Their functionality (i.e., the number of hydroxyl groups) increases with the increasing degree of methylene bridging. Networks are formed by a hydroxyl–epoxide reaction. Due to their high functionality, the novolac molecules behave as "chain concentrators" that induce regions of higher crosslink density. Therefore, epoxy networks with a heterogeneous structure are formed that contain both highly crosslinked rigid structures from the novolac oligomers and flexible segments from the aliphatic epoxy resin.

The higher toughness and lower brittleness of epoxy-novolac systems in comparison to other epoxies show them to be well suited for a systematic investigation of the molecular orientation behavior of epoxy resins by rheooptical FTIR spectroscopy. This article deals with such a study on epoxies made of the diglycidyl ether of butanediol (DGEB) and the bisphenol A novolacs. The effect of temperature and strain rate was studied. Furthermore, the epoxy resins were subjected to successive loading–unloading cycles. The orientation and relaxation phenomena occurring during such cyclic deformation experiments is reported.

EXPERIMENTAL

Sample Preparation and Characterization

Bisphenol A novolacs were synthesized from bisphenol A and paraformaldehyde in a melting process as described by Strehmel et al.[21] Two samples with different degrees of methylene bridging were prepared. Some data of their characterization are given in Table I. The chemical structure is shown in Figure 1. The novolac samples were kindly supplied by Dr. V. Strehmel, University of Halle.

Epoxy networks were prepared from DGEB and the novolacs using imidazole as an accelerator. DGEB (Aldrich) was purified by distillation.[22] Imidazole (Merck) was recrystallized from a benzene-ethanol mixture.[21] The novolac was melted, and DGEB was added in the stoichiometric ratio. Epoxy resin, novolac, and accelerator (0.65 mol % imidazole relative to epoxy groups) were stirred until the mixture became homogeneous. Then the mixture was vacuum degassed for a few minutes.

For the preparation of thin epoxy films suited for both mid-IR spectroscopy and mechanical measurements, the mixture was cast between

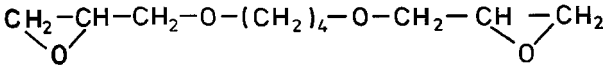

(a)

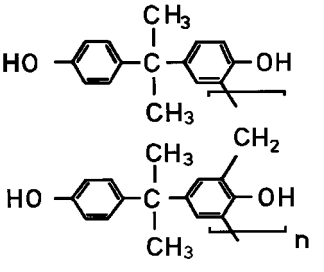

(b)

Figure 1 Chemical structures of (a) the diglycidylether of butanediol (DGEB) and (b) the novolacs on the basis of bisphenol A.

preheated steel plates. These plates were covered with release films from poly(tetrafluoroethylene-*co*-hexafluoropropylene) (FEP, Richmond Aircraft Products). The steel device ensures controllable diversion of the heat of reaction and guarantees isothermal curing. The samples were crosslinked in a two-stage process. They were first cured at 130°C for 5 h and then postcured at 170°C for 30 min. After cooling to room temperature, the epoxy films were carefully peeled off the release film and checked for possible defects by a light microscope. Their thickness was determined by using a digital length gauge (resolution 0.5 μm). For rheooptical experiments, only film pieces with a constant thickness (within the limits of the instrument resolution) and without any visible flaws were used. The typical thickness of the samples was 10 μm. They were cut with a scalpel to gauge dimensions of 12 $\times$ 8 mm.

The final conversion of the epoxide in the cured networks was verified by near-IR (NIR) spectroscopy. Samples were prepared by pouring a part of the mixture used for film casting into small preheated steel frames (2 mm thick) treated with a release agent (Frekote 44-NC). The frames covered with FEP release films were placed between steel plates preheated to the curing temperature as well. Crosslinking proceeded simultaneously to film curing under the same conditions. NIR spectra were obtained using a Bruker IFS 66 FTIR spectrometer. For monitoring the epoxide consumption, the band at 2205 nm (4535 cm^{-1}) in the NIR spectrum was used, which is due to a combination of the CH stretching vibration at 3050 cm^{-1} with the CH_2 deformation mode at 1460 cm^{-1}.[23] After curing in the two-stage process, this absorption completely vanished (i.e., no unconverted epoxide functionalities remained in the cured network).

The glass transition temperatures (T_g) of the cured samples were measured[22,24] with a Perkin–Elmer DSC 7 in the range of -70 to 200°C at a heating rate of 10°C min^{-1}.

The average molecular weight between crosslinks (M_c) was determined by dynamic-mechanical analysis (DMA) using a Rheometrics Dynamic Analyzer RDA II. Samples were torqued at oscillating frequencies of 0.1, 1, and 10 Hz with a strain amplitude of 0.2%. The temperature range from -80 to 150°C was scanned with a heating rate of 10°C min^{-1}. The M_c values were calculated from the equilibrium modulus G_{eq} at T_g + 40°C by using the expression $G_{eq} = \rho RTM_c^{-1}$, where ρ is the density of the epoxy resins.[24] The glass transition temperatures and network densities are given in Table II.

Table II Glass Transition Temperatures[22,24] and Network Densities of DGEB/Novolac Networks

Novolac	DNL 7.5	DNL 15
T_g (°C)	50.5	57
M_c (g/mol)	720	530

Rheooptical FTIR Spectroscopy

The rheooptical measurements were carried out using a variable temperature electromechanical stretching machine developed by Siesler.[25] Polymer films can be studied in uniaxial deformation and relaxation experiments at variable strain rates and under controlled temperature conditions with an accuracy of $\pm$0.5°C. In this study, most stretching experiments were performed with a loading rate of 0.005 mm s^{-1}. Some samples were elongated with the double strain rate. The stretching apparatus was installed in the sample compartment of a Bruker IFS 66 FTIR spectrometer equipped with a mercury-cadmium-telluride detector cooled by liquid nitrogen. The polarization of the incident radiation (parallel and perpendicular with respect to the stretching direction) could be rapidly changed by 90° rotation of a gold wire grid polarizer (Specac) mounted in an electromechanical rotator. The change of the polarization direction was automatically initiated by the last scan of each spectrum. The rheooptical experimental setup was described in detail in a previous article.[12]

Single-channel spectra with alternating polarization directions were taken successively in 6.5-s intervals. For each spectrum 10 scans were coadded. Absorbance spectra with 2 cm^{-1} resolution were calculated after completion of the experiment using two spectra of the polarizer recorded with different polarization directions as references.

The FTIR spectrum of a DGEB/bisphenol A novolac film taken before deformation and without polarizer is plotted in Figure 2.

The orientation of a polymer chain can be described by an orientation distribution function $f(\theta,\phi,\psi)$.[26,27] The segmental orientation in uniaxially oriented samples is given by the second moment of this distribution function as

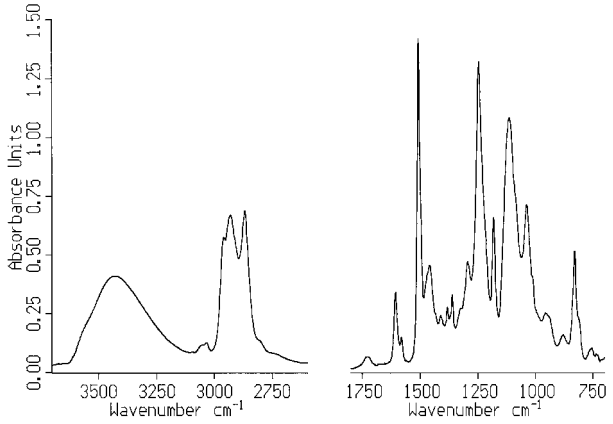

Figure 2 FTIR spectrum of DGEB/DNL 7.5.

$$\langle P_2(\cos\theta)\rangle = \frac{3\langle\cos^2\theta\rangle - 1}{2} \quad (1)$$

where θ is the average angle between the chain axis and the stretching direction. The orientation coefficient $\langle P_2(\cos\theta)\rangle$ is related to the dichroic ratio $R = A_\parallel/A_\perp$ by the expression

$$\langle P_2(\cos\theta)\rangle = \frac{(R-1)(R_0+2)}{(R+2)(R_0-1)} \quad (2)$$

$A_\parallel$ and $A_\perp$ are the absorbances measured with radiation polarized parallel and perpendicular to the stretching direction. $R_0 = 2\cot^2\alpha$ is the theoretical dichroic ratio for perfect uniaxial alignment of the chains. The angle α is spread between the transition moment vector of the vibrational mode considered and the local chain axis segment.

The assignment of the absorption bands evaluated for the determination of the orientation coefficient has to be well known in order to deduce the correct angle α. In the spectra of the DGEB/novolac resins, the bands that are attributed to various vibrations in the backbone of the chains (e.g., the carbon–carbon and ether bonds) do not show any variation of the dichroic ratio during deformation of the sample. The absorptions at 1460 and 3400 cm^{-1} exhibit perpendicular dichroism. However, the respective transition moment angles α are not known. The transition moment corresponding to the CH_2 stretching vibrations at 2930 and 2872 cm^{-1} are known to be situated perpendicularly to the local chain axis segment ($\alpha = 90°$).[28] The latter band (υ_s CH_2) was used for the calculation of $\langle P_2(\cos\theta)\rangle$.

Orientation measurements by the IR dichroism technique require band absorbances to be sufficiently low to permit the use of the Lambert–Beer law. For epoxy films with a thickness of about 10 μm, this condition is fulfilled. Only bands with absorptions smaller than 1.0 were evaluated for calculating the orientation coefficient. The absorbances $A_\parallel$ and $A_\perp$ are based on integral intensities. All spectra were normalized to the intensity of a reference band in order to compensate for the decreasing sample thickness during elongation. The band at 1610 cm^{-1} assigned to the υ (C═C) stretching mode of the paradisubstituted benzene ring in the diphenylpropane unit of the novolacs was found to be a suitable reference band.

RESULTS AND DISCUSSION

Deformation in Rubbery State

The deformation and orientation behavior of the novolac cured epoxy networks was first investigated in the rubbery state. Samples were uniaxially stretched at a loading rate of 0.005 mm s^{-1} until fracture of the sample. The stress–strain curve of DGEB/DNL 7.5 at $T_g + 20°C$ is shown in Figure 3(a). The second Legendre polynomial $\langle P_2(\cos\theta)\rangle$ calculated from the FTIR spectra recorded simultaneously is plotted versus strain in Figure 3(b). In comparison with other polymers studied by rheooptical FTIR spectroscopy, only small changes of the dichroic ratio and, consequently, low values for $\langle P_2(\cos\theta)\rangle$ as a measure of orientation were found for the epoxy resins.

The stress shows a slightly nonlinear dependence on the strain, which is typical for most rubbers.[4,8,9] However, highly crosslinked epoxies with short network chains like those studied here do not behave like ideal elastomers; the influence of the non-Gaussian character and the finite extensibility of the chain segments has to be taken into consideration.[29]

The orientation depends nearly linearly on the strain. Similar orientation behavior was also observed for epoxy/amine networks prepared from DGEBA and polyetheramines when being investigated above the glass transition temperature[12] and for the poly(oxytetramethylene) soft segments in polyether-urethanes.[30]

The deformation process of crosslinked polymers in the rubbery state is based on the uncoiling and extension of individual network chain segments by rotations about their skeletal bonds.

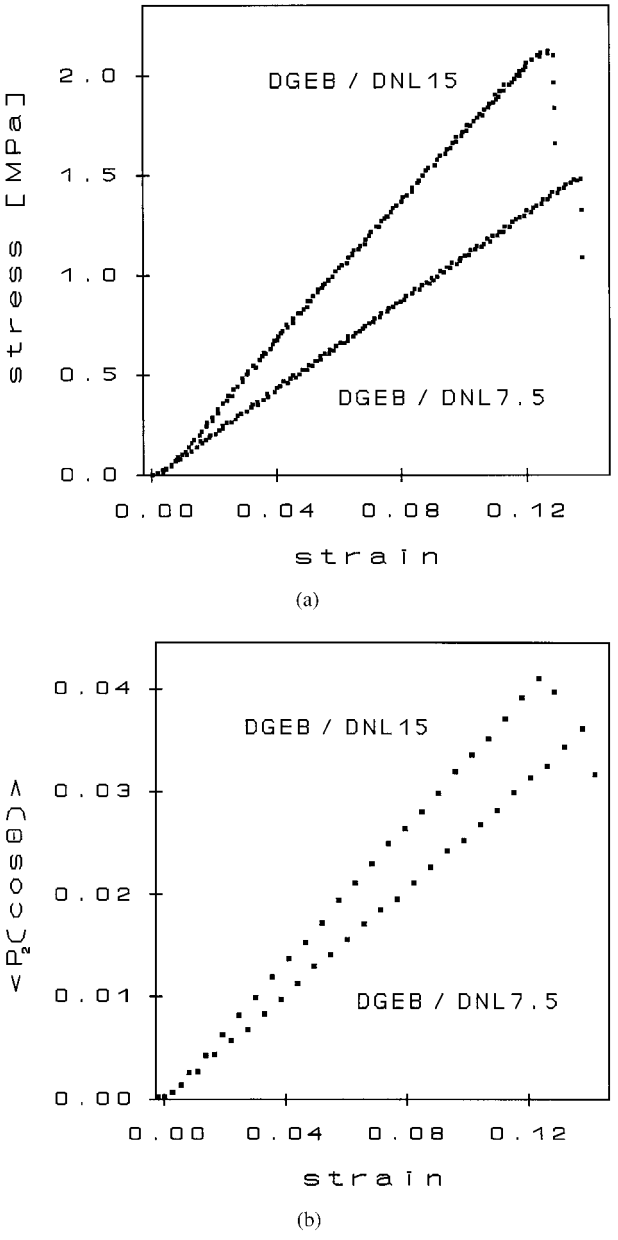

Figure 3 Deformation of DGEB/novolac resins at T_g + 20°C: (a) stress–strain curves and (b) orientation parameter $\langle P_2(\cos\theta)\rangle$.

In the FTIR spectrum of the DGEB/novolac systems, only bands belonging to the CH_2 stretching vibrations show a changing dichroism on deformation. This indicates that mainly the methylene sequences coming from the DGEB are extended whereas the rigid diphenylpropane units in the novolac molecules largely resist the deformation. As far as permitted by the geometric constraints, the uncoiled chain segments become oriented, which is reflected in a continuous increase of $\langle P_2(\cos\theta)\rangle$.

The slope of the orientation function of the both epoxy/novolac resins depends on their network densities: in the DGEB/DNL 15, more diphenylpropane units are linked by methylene bridges. These links reduce the ability of the network chains to translate against each other. Therefore, the aliphatic segments become more rapidly uncoiled and extended than in DGEB/DNL 7.5 having a lower degree of crosslinking.

The uncoiling and orientation of the network chain segments is connected with conformational changes. Many results of the observation of such changes in stretched polymers by IR spectroscopy have already been reported.[1,3,8,26] In contrast, during the deformation of the novolac cured epoxies in the present study, as well as for DGEBA/amine resins investigated previously,[12] changes in the spectra indicating conformational transitions induced by the deformation process could not be detected. This is caused by the lack of specific conformation-sensitive vibrational bands. The IR spectrum of the epoxies studied is dominated by the very strong absorbances of the stiff diphenylpropane structures whereas deformation is predominantly localized in the flexible aliphatic chains. In these chains there are numerous possibilities for rotation about carbon–carbon or carbon–oxygen bonds. However, the few absorptions attributed to these chain segments are independent of changing conformation.[31] Therefore, the conformational changes cannot be directly observed by FTIR spectroscopy.

Although the direct evidence for changes in the conformational distribution failed, it should be emphasized that conformational changes of the chain segments are the basis for the storage of mechanical energy transferred to the network during the deformation process. Investigations of epoxy resins subjected to successive loading–unloading cycles in their rubbery state indicate the occurrence of conformational changes. These results are reported in detail in the last part of this article.

Deformation in Glassy State

Deformation and orientation of the DGEB/novolac epoxies were also studied below the T_g. Again, the films were stretched with a strain rate of 0.005 mm s^{-1}. The stress–strain diagram and $\langle P_2(\cos\theta)\rangle$ of DGEB/DNL 7.5 at T_g − 20°C are shown in Figure 4.

Both curves differ completely from the behavior of the corresponding curves at $T > T_g$. The

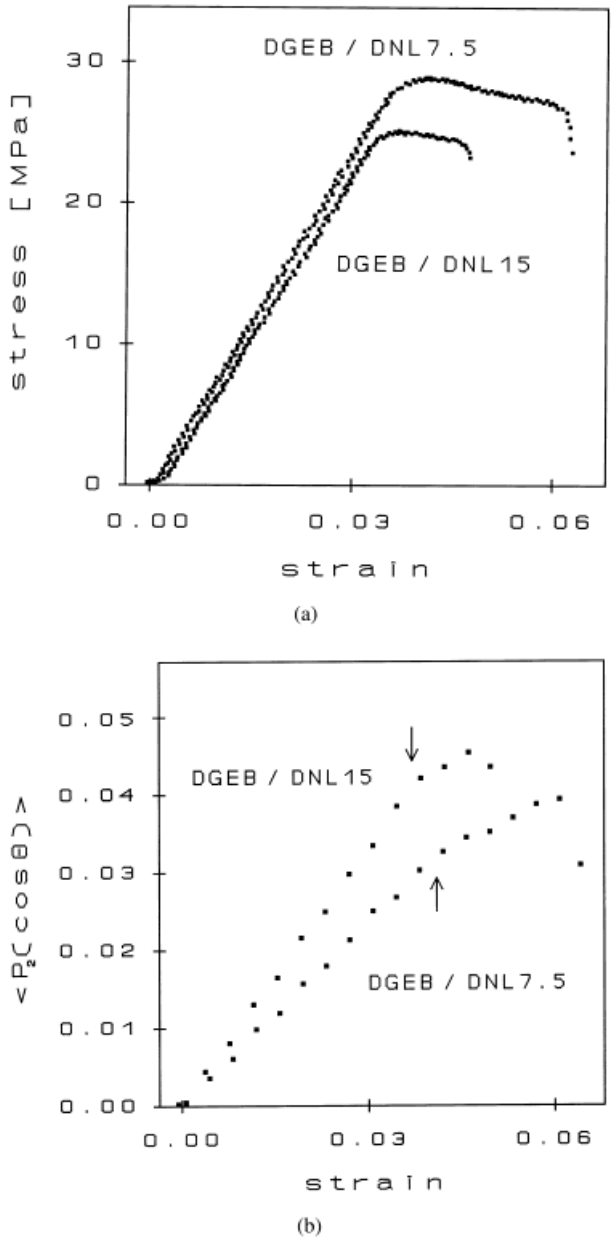

Figure 4 Deformation of DGEB/novolac resins at T_g − 20°C: (a) stress–strain curves and (b) orientation parameter $\langle P_2(\cos\theta)\rangle$. The arrows mark the position of the yield point.

stress–strain plot is characterized by the appearance of the yield point. The orientation rises nearly linearly with increasing strain before yielding. On going through the yield point, $\langle P_2(\cos\theta)\rangle$ changes its slope. The strain at this bend coincides with the yield strain. After the yield point, a slower increase of the orientation can be observed.

Analogous results were obtained for the orientation behavior of DGEBA/polyetheramine systems in the glassy state.[13] The curves of the orientation parameter of these epoxies show the same typical bend in the vicinity of the yield point.

The change of the slope in the yield region indicates a significant change of the molecular orientation behavior and has to be related to the mechanism of plastic deformation. Epoxy resins can undergo plastic deformation, although they often show macroscopic brittle behavior. Physical descriptions of the plastic flow of amorphous polymers at a molecular level were developed by Argon[32] and Bowden and Raha.[33] Oleinik[34,35] and Caux et al.[36] proposed models for a qualitative description of the nonelastic deformation in terms of plastic shear deformation. These models were applied to the discussion of rheooptical data of epoxy resins at temperatures below the T_g.[13,14]

From a phenomenological point of view, plastic deformation of glassy polymers may be envisioned as the nucleation and growth of specific defects, which store the elastic energy without significant changes of the conformational distribution. The defects originate from molecular slip, glide, and rotation events induced by the shear component of the applied stress. Thermodynamically, the plastic shear defects are metastable states. Repeated nucleation of such defects predominates prior to the yield point.

The energy of the individual defects increases more and more during further deformation until the internal energy stored in the plastic shear defects reaches a plateau. Macroscopically, this stage corresponds to the yield point. The shear defects terminate their growth and begin to transform. This relaxation process leads to a local conformational rearrangement of the chain segments inside the defects. The conformational transitions conserve the microscopic displacement in the defects, but at a considerably lower level of energy.

The main contribution to an increase of the orientation results from nucleation and growth of the plastic shear defects. Due to molecular slippage processes the matter in the defects becomes highly oriented. The repeated formation of defects up to the yield point leads to a rapidly growing defect concentration. The orientation function shows a strong slope. After passing through the yield region, the defect concentration effectively does not increase any more due to the simultaneous conversion of shear defects by conformational rearrangements. The conformational transitions predominantly fix the degree of orientation already achieved. Accordingly, the orientation in the epoxy films is growing

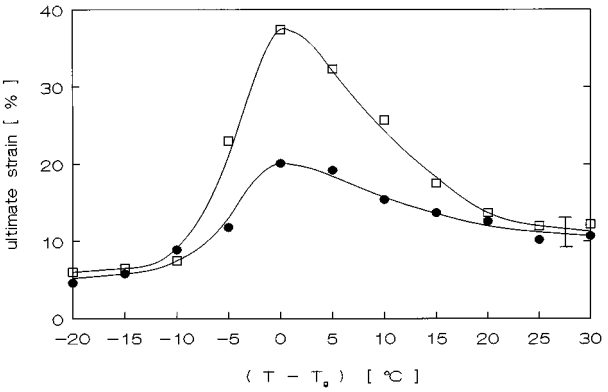

Figure 5 Ultimate strain of DGEB/novolac resins dependent on ($T - T_g$): (□) novolac DNL 7.5 and (●) novolac DNL 15.

slower beyond the yield point, and the curve of $\langle P_2(\cos\theta)\rangle$ changes its slope in this region.

As discussed above, the changes in the conformational distribution cannot be directly observed, but indirect evidence can be obtained also in the glassy state from cyclic deformation experiments.

Temperature Dependence of Deformation Behavior of DGEB/Novolac Epoxies

Mechanical Properties

The temperature dependence of the mechanical properties and the orientation behavior of the novolac cured epoxies was investigated in the range of $T_g - 20$°C to $T_g + 30$°C. For each temperature, 5–10 rheooptical measurements were performed. The ultimate strain ϵ_b and strength σ_b and the tensile modulus E of the DGEB/bisphenol A novolac networks are plotted versus ($T - T_g$) in Figures 5–7.

The temperature dependence of the elongation at break (Fig. 5) shows a clear maximum at the T_g. Ochi et al.[37] also observed such a maximum for a biphenol-type epoxy resin cured by a phenol novolac. The same behavior was found by Gupta et al.[38] for DGEBA/diamine epoxies. This phenomenon is well known in the field of failure mechanics of polymer materials. In the glasslike state, the epoxy films are quite brittle. During tensile tests well below the glass transition temperature, they broke before yielding at strains up to 4%. In the viscoelastic state, the samples show an increased ductility and consequently reach their maximum extensibility. In the rubbery state, the intermolecular forces nearly vanish. The material is no longer able to support high loads and again breaks down at lower extensions.

The maximum extensibility also corresponds to the network density. The epoxies cured by the novolac DNL 7.5 have a higher M_c value; consequently, their elongation at break is higher than for the networks on the basis of DNL 15. The higher amount of methylene links in the latter strongly restricts the mutual mobility of the chain segments past each other. A similar dependence of the ultimate strain on the network density of epoxy novolac systems was reported by Madsen and Foister.[18]

The tensile modulus was calculated from the initial linear part of the load–elongation curve. Results are shown in Figure 6. The modulus shows a characteristic decrease with increasing temperature in the glass transition region. Moreover, the influence of the network density can again be clearly seen. DGEB/DNL 15, which is the sample with the higher crosslink density, has the lower modulus at temperatures below the glass transition and the higher modulus above it. In the glassy state, this reflects a close correlation of the tensile modulus with the molecular packing density or the free volume, respectively. The smaller the free volume, the higher the packing density. The intermolecular packing is the predominant factor determining the modulus below the T_g. Closer packing of the molecules results in a higher tensile modulus and a larger yield strain. Due to the higher content of methylene bridges in DNL 15 and the stiffness of the diphenylpropane segments, the molecular packing in epoxy resins made from this novolac is more strongly impaired than in those based on DNL 7.5, which is reflected in a lower tensile modulus and a smaller yield strain of the former samples. In DGEB/DNL 15, yielding at $T_g - 20$°C occurs at an elongation of $3.7 \pm 0.2\%$, whereas the yield strain in DGEB/DNL 7.5 was found to be $4.1 \pm 0.2\%$.

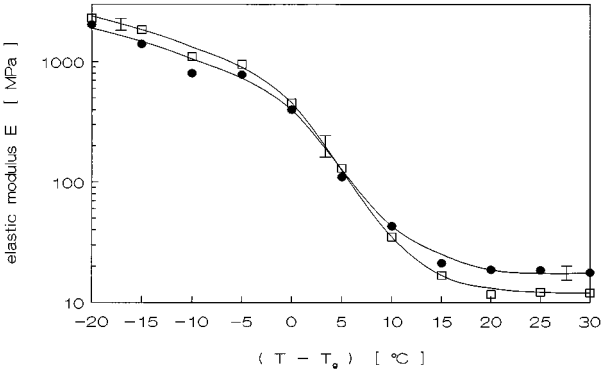

Figure 6 Dependence of the elastic modulus E on ($T - T_g$): (□) novolac DNL 7.5 and (●) novolac DNL 15.

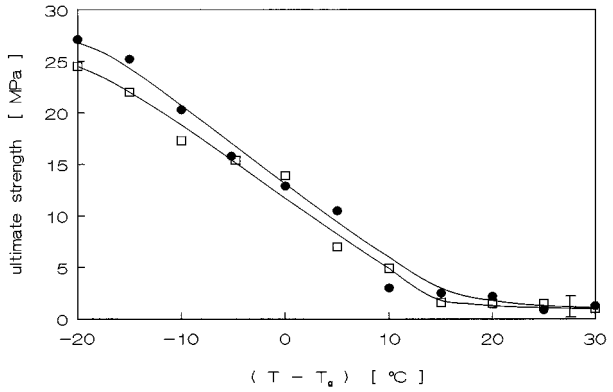

Figure 7 Ultimate strength of DGEB/novolac resins dependent on ($T - T_g$): (□) novolac DNL 7.5 and (●) novolac DNL 15.

Above the T_g the rubberlike elastic deformation is associated with changes in molecular conformation and the intermolecular forces no longer play a dominant role. Instead, the modulus is determined by the network density. The higher modulus of the stronger crosslinked sample arises from the greater constraints to mobility because of the pinning of the molecules at the crosslink sites.

The same interrelations between the tensile modulus of epoxy resins and its dependence on temperature and the packing or network density, respectively, were reported by numerous authors.[17,29,38–40]

The temperature behavior of the tensile modulus is reflected in the variation of the ultimate strength with temperature shown in Figure 7. The similarity of the dependencies of σ_b and E on ($T - T_g$) is quite obvious. The strength also decreases remarkably in the glass transition region and shows very low values for rubbery networks. Analogous results for the temperature dependence of the strength were already obtained for various amine[36,38,41] and novolac[37] cured epoxy resins. At temperatures below the T_g, the tensile strength is governed by the intermolecular packing density; the resistance to deformation arises from intermolecular forces. In the vicinity of the glass transition, the intermolecular cohesion decreases more and more. In the rubbery state, the mechanical behavior is dominated by the crosslink density.

Orientation Behavior

Figure 8 shows the temperature dependence of the degree of orientation at two fixed strains (5 or 12%, respectively) for both DGEB/novolac resins. Again, the CH_2 stretching vibration at 2872 cm^{-1} (υ_s CH_2) was used for the calculation of $\langle P_2(\cos \theta)\rangle$. As already mentioned, bands assigned to the backbone or the aromatic novolac segments do not show any changing dichroism on deformation; mainly the aliphatic chains coming from the DGEB become oriented.

The gradual decrease of the degree of orientation in the glass transition region is quite conspicuous. At equal strain, the orientation below the T_g is much higher than above the T_g. Zhao et al.[5,6] studied the temperature dependence of the orientation function during the deformation of poly(methyl methacrylate) (PMMA) at $T > T_g$ and also found such behavior. Jasse and Koenig[1] observed a steep increase of the orientation in polystyrene during extension at the T_g, whereas it grew slowly when deformation was performed at $T_g + 10$°C.

The temperature dependence of $\langle P_2(\cos \theta)\rangle$ resembles that of the tensile modulus. This indicates that both occur for the same reason. Consequently, the change of the orientation in the glass transition region is associated with the change of the molecular mechanism of deformation. At temperatures below the T_g, the deformation behavior is governed by strong intermolecular forces. The orientation is dominated by the formation of plastic shear defects with highly oriented matter inside. In the vicinity of the glass transition, the intermolecular cohesion between the chain segments decreases more and more with increasing temperature. The degree of orientation also increases more slowly. In the rubbery state, the orientation

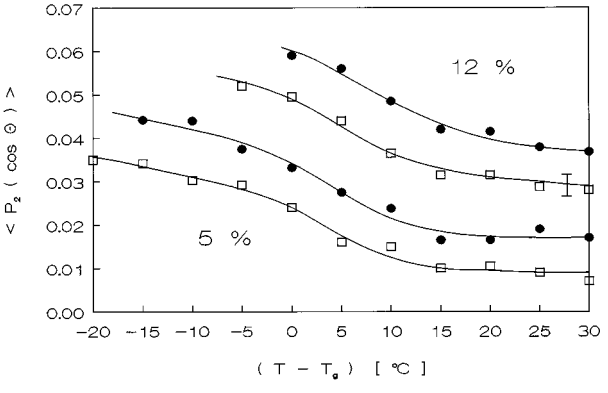

Figure 8 Dependence of the orientation parameter $\langle P_2(\cos \theta)\rangle$ at 5 or 12% strain on ($T - T_g$): (□) novolac DNL 7.5 and (●) novolac DNL 15; strain rate 0.005 mm s^{-1}.

behavior is determined by conformational changes that contribute less to $\langle P_2(\cos\theta)\rangle$ than the plastic shear defects in the glassy resins.[13]

Moreover, it can be clearly seen that at temperatures both above and below the glass transition, the orientation in networks containing the novolac DNL 15 is somewhat higher than in the epoxies based on DNL 7.5. For the rubbery networks, this can be attributed to the different network densities. At a given strain, short network chains are more extended than longer ones. Amram et al.[4] observed such behavior for natural and synthetic rubbers with different degrees of crosslinking. In the epoxy/novolac networks, the situation is something different. Due to their high average functionality, the novolac molecules act as "chain concentrators," forming rigid blocks with several aliphatic chain segments attached to them. The mutual mobility of these attached chains against each other is strongly restricted. Thus, they become rapidly oriented on increasing deformation of the network. The functionality of the novolac molecules rises together with the degree of bridging. With increasing functionality, more and more aliphatic chain segments are linked to such a nearly undeformable novolac molecule. Due to the stronger constraints to mobility, the orientation of the aliphatic chains increases more rapidly with the rising degree of crosslinking (i.e., the orientation in DGEB/DNL 15 is higher than in DGEB/DNL 7.5).

The behavior of the orientation parameter closely corresponds to the ultimate strain of the two networks. The chains in the higher crosslinked networks (i.e., those containing DNL 15) become not only more rapidly extended on deformation, but they also earlier reach their finite extensibility earlier; the networks break at lower strain (see Fig. 5).

Below the glass transition temperature, the epoxies on the basis of the novolac DNL 15 show a higher segmental orientation, too. The molecular slip and glide motions responsible for deformation in the glassy state can occur more easily if sufficient free volume is available.[34–36] Accordingly, stronger packing constraints enhance the local segmental mobility. The higher the content of methylene bridges, the more impaired is the intermolecular arrangement by steric hindrance effects. Therefore, epoxy samples with DNL 15 are less resistant to plastic deformation than those containing DNL 7.5, which is consistent with the observed lower tensile modulus and smaller yield strain of the former. The extent of plastic deformation is reflected in the degree of orientation in the stretched film. Consequently, the slope of the orientation coefficient versus strain is larger for the more loosely packed system DGEB/DNL 15, and its curve of $\langle P_2(\cos\theta)\rangle$ versus $(T - T_g)$ lies above that of the other resin in the glassy state.

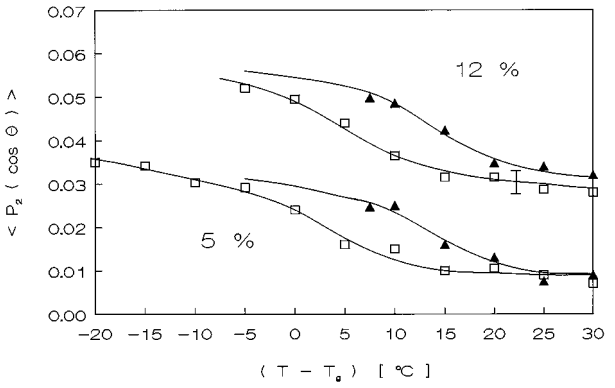

Figure 9 Orientation parameter $\langle P_2(\cos\theta)\rangle$ versus $(T - T_g)$ at different strain rates: (□) 0.005 mm s^{-1} and (▲) 0.01 mm s^{-1}; orientation at 5 or 12% strain; sample DGEB/novolac DNL 7.5.

Influence of Strain Rate on Orientation Behavior

Due to the similarity of the temperature dependencies of the tensile modulus and the orientation parameter, a dependence of the orientation on the strain rate can be expected. Figure 9 plots the orientation coefficient $\langle P_2(\cos\theta)\rangle$ of DGEB/DNL 7.5 versus $(T - T_g)$ for two different loading rates. Investigations were performed at 0.005 and 0.01 mm s^{-1} (initial length of the sample 12 mm). Higher strain rates could not be studied because in this case only very few spectra were recorded up to the early rupture of the film. Moreover, an extension of the study to lower temperatures was also not possible for the same reason.

With increasing strain rate, the curve of $\langle P_2(\cos\theta)\rangle$ versus $(T - T_g)$ is shifted to higher temperatures. On doubling the strain rate, the shift is about 10°C. An analogous behavior of the orientation was observed by Zhao et al.[5,6] during the rheooptical investigation of PMMA at $T > T_g$ with loading rates between 0.008 and 0.115 s^{-1}.

As expected, the dependence of $\langle P_2(\cos\theta)\rangle$ on the strain rate corresponds to the frequency dependence of the modulus, which can also be realized, for example, from the behavior of the dynamic shear modulus in DMA measurements where the curves of the modulus obtained at

higher torsional frequency are also shifted to higher temperatures. These shifts are caused by the stronger hindrance of the relaxation at a higher loading rate or frequency, respectively (i.e., the molecular relaxation processes are progressively less able to respond to an external influence such as the extension of the sample). This behavior is reflected by the time–temperature equivalence of the viscoelastic properties of amorphous polymers that is expressed in the well-known Williams–Landel–Ferry equation. With increasing distance to the glass transition, the difference between the orientation at the two strain rates vanishes more and more.

Molecular Orientation Phenomena during Cyclic Deformation

So far, the molecular deformation behavior of the novolac cured epoxies was studied during continuous stretching processes that were carried out up to the failure of the film. However, rheooptical FTIR spectroscopy also offers the possibility to obtain comprehensive information on molecular orientation and relaxation phenomena occurring during repeated elongation and recovery of the sample. The investigation of the reversibility of the orientation during such loading–unloading cycles can contribute to a deeper insight into the mechanism of polymer deformation at a molecular level both above and below the glass transition temperature. Moreover, specific cyclic deformation experiments can be designed to obtain indirect spectroscopic evidence for the occurrence of conformational changes during elongation whose direct observation failed due to the lack of conformation-sensitive vibrational bands in the IR spectrum of the epoxy/novolac resins.

Cyclic Deformation of Rubbery Epoxy Networks

At first the molecular orientation behavior of a DGEB/DNL 7.5 epoxy network was investigated during cyclic deformation in the rubbery state. At T_g + 20°C, five successive loading–unloading cycles were performed at a constant stretching and recovery rate of 0.005 mm s^{-1}. The stress–strain curve is plotted in Figure 10(a). The increase and the decrease of the orientation was simultaneously obtained by IR spectroscopy [Fig. 10(b)].

In each elongation–recovery cycle, the epoxy film was stretched to a higher maximum strain than in the preceding one. The stress–strain

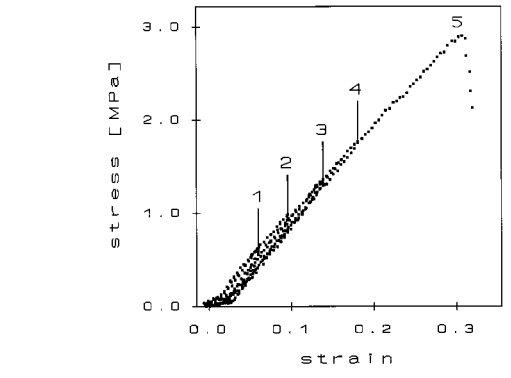

(a)

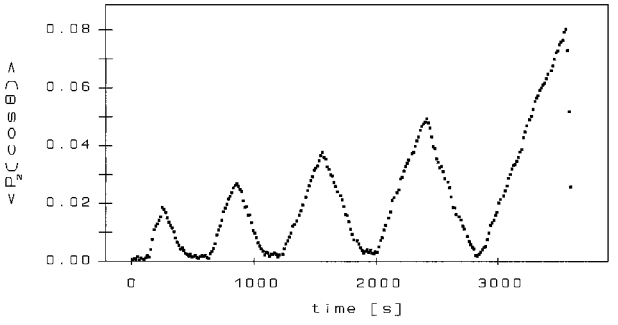

(b)

Figure 10 Cyclic deformation of DGEB/DNL 7.5 at T_g + 20°C, five successive loading–unloading cycles: (a) stress–strain curve and (b) orientation parameter $\langle P_2(\cos\theta)\rangle$ versus time.

curves again show a slightly nonlinear behavior that is in contrast to the linear stress–strain dependence observed during the cyclic deformation of rubbery networks on the basis of DGEBA and polyetheramine.[12] The curves for elongation and recovery are identical without any hysteresis effect. Furthermore, the curves of the consecutive cycles are nearly in congruence as well. These results indicate that fatigue of the network by extensive chain rupture in overstrained segments obviously does not occur. Upon unloading, a minor remaining elongation of the samples can be observed. This could be caused by some irreversible disentanglement or a slight slip of the film specimen on the grips.

The orientation behavior that is plotted versus time in Figure 10(b) corresponds exactly to the stress–strain curve. The rise and fall of $\langle P_2(\cos\theta)\rangle$ perfectly coincides with the increase and decrease of the strain. When the sample is unloaded, the orientation completely vanishes without any time lag to the disappearance of the stress. These results clearly prove the total reversibility of the

molecular orientation in novolac cured epoxy resins above the glass transition temperature.

The observed behavior of the molecular orientation is a strong indication that conformational transitions occur during the elongation of epoxy networks. The increase and decrease of $\langle P_2(\cos\theta)\rangle$ corresponds to the excitation and relaxation of conformational states during loading and unloading of the film. The complete reversibility of the molecular orientation on unloading the sample is in accordance with the total relaxation of the excited conformational states to their equilibrium distribution in rubbery networks. Consequently, the results of the cyclic deformation experiment confirm the occurrence of conformational changes indirectly.

Cyclic Deformation in Glassy State

Complementary to the rubbery state, molecular orientation and relaxation phenomena were also studied during a specific elongation–recovery sequence of DGEB/DNL 7.5 below the glass transition temperature. The stress–strain plot and the second moment of the orientation distribution function are shown in Figure 11.

Initially, the sample was subjected to two successive loading–unloading cycles at $T_g - 20°C$. During the unloading of the film, a hysteresis is observed in the stress–strain diagram. The strain does not completely vanish; a small permanent elongation remains in the sample after the disappearance of the stress. The effect of the incomplete recovery of the shape of the sample becomes even more noticeable after the second deformation cycle.

The orientation also only partly relaxes when the specimen is unloaded. After a rapid decrease of $\langle P_2(\cos\theta)\rangle$ at the beginning of the unloading process, the relaxation of the orientation levels off and leaves a considerable residual orientation in the sample. Almost no relaxation of this orientation can be discerned. The plateau in the curve of $\langle P_2(\cos\theta)\rangle$ is even higher after the next loading–unloading cycle. The increasing permanent orientation causes a self-reinforcement of the sample that is reflected in a drastic increase of the elastic modulus in the second cycle to about twice the value of the initial modulus. Both phenomena, the remaining orientation and the self-reinforcement, correspond to the permanent elongation of the sample after unloading. Moreover, the relaxation rate of the orientation is reduced in the preoriented sample during the decay phase in the second cycle.

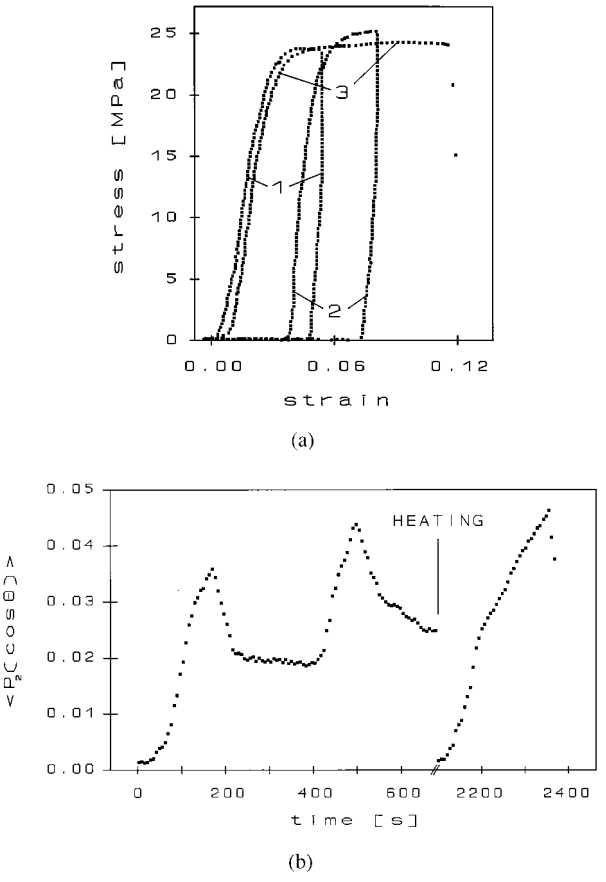

Figure 11 Cyclic deformation of DGEB/DNL 7.5 at $T_g - 20°C$ with heating of the sample to $T_g + 25°C$ between the second and third cycle: (a) stress–strain curve and (b) orientation parameter $\langle P_2(\cos\theta)\rangle$ versus time.

The phenomena observed during this cyclic deformation experiment are in accordance with the proposed molecular mechanism of deformation of glassy polymers[32–35] that was discussed above. The increase of the orientation mainly results from the nucleation and growth of the plastic shear defects. These defects are metastable states; they are stable under stress only. Therefore, their contribution to $\langle P_2(\cos\theta)\rangle$ rapidly relaxes when the stress vanishes. However, after passing through the yield point region, a gradual conversion of shear defects by conformational transitions starts to occur, which in part conserves the degree of orientation. The conformational rearrangements are irreversible below the glass transition temperature. Accordingly, after the exponential decay of the contribution of the shear defects, a plateau remains in the plot of $\langle P_2(\cos\theta)\rangle$ that is due to the conformational changes.

In order to prove that the orientation plateau in the sample is really caused by conformational changes, the reversibility of the orientation in the rubbery state was tested. After the second elongation–recovery cycle at $T_g - 20$°C, the unloaded sample was heated to 25°C above the T_g. As soon as the glass transition temperature was reached, the plateau in the curve of $\langle P_2(\cos \theta)\rangle$ vanished immediately, which is consistent with the relaxation of the excited conformational states. This means that the occurrence of conformational changes during the deformation of novolac cured epoxies is also confirmed for temperatures below the glass transition.

When the previous temperature of deformation was attained after cooling, the sample was elongated again until fracture of the film. The behavior of the epoxy film sample during this stretching completely resembles that in the initial deformation cycle. In particular, the permanent increase of the sample length nearly completely disappeared; and the elastic modulus returned to its original value, which once again reflects the erasure of the orientation during the heating to above the T_g. The slope of $\langle P_2(\cos \theta)\rangle$ during the third cycle is also almost the same as during the first elongation. The recovery of the initial sample shape and the unchanged slope of the curve of the orientation coefficient both indicate that under the conditions of this cyclic deformation experiment, chain scissions and other fatigue effects were apparently only of minor importance in the glassy epoxy sample, too.

CONCLUSIONS

The molecular orientation and relaxation behavior of novolac cured epoxy resins during their uniaxial deformation was monitored by rheooptical FTIR spectroscopy. Investigations were performed in both the rubbery and glassy state of the epoxies.

Upon deformation below the T_g, only bands assigned to the methylene sequences were found to show a changing dichroism. This indicates that mainly the chain segments coming from the DGEB are extended whereas the rigid diphenylpropane units in the novolac molecules largely resist the deformation. The orientation depends nearly linearly on the strain. Moreover, it is influenced by the network density: in DGEB/DNL 15, the sample with the higher degree of methylene bridging and, accordingly, with the more densely crosslinked network, the aliphatic segments become more rapidly uncoiled and extended with increasing elongation.

In the glassy state, the orientation function was found to show an abrupt change of its slope in the yield point region. This phenomenon indicates a significant change of the molecular orientation behavior and was discussed with respect to the mechanism of plastic deformation. The bend in the curve of $\langle P_2(\cos \theta)\rangle$ was attributed to the beginning conversion of plastic shear defects by complex conformational rearrangements.

Moreover, the temperature dependence of the molecular deformation behavior was studied. The elongation at break was found to have a clear maximum at the T_g. The tensile modulus shows a characteristic decrease at the glass transition. The behavior of the ultimate strength is similar to that of the modulus. The degree of orientation also decreased gradually in the glass transition region. The mechanical properties and the orientation are both strongly influenced by the network density.

The changes of the orientation behavior and the mechanical properties in the glass transition region are associated with the change of the molecular mechanism of deformation. At temperatures below the T_g, the deformation behavior is governed by intermolecular forces. In the vicinity of the glass transition, the intermolecular cohesion decreases more and more. In the rubbery state, the properties are dominated by the crosslink density.

The molecular orientation behavior was also investigated as to its dependence on the rate of stretching. With an increasing strain rate the curve of $\langle P_2(\cos \theta)\rangle$ versus $(T - T_g)$ is shifted to higher temperatures because the molecular relaxation processes increasingly fall behind the macroscopic process (i.e., the extension of the sample).

Additionally, epoxy films were subjected to successive loading–unloading cycles above and below the glass transition temperature in order to study the reversibility of the orientation. The investigations show that the orientation is completely reversible in the rubbery state whereas it only partly relaxes at temperatures below the T_g. However, it can be annealed by heating the sample to above the glass transition temperature. Moreover, the results of the two cyclic deformation experiments confirmed the occurrence of conformational changes during the deformation of the novolac cured epoxies. Such changes had not been directly observed in the spectrum of the epoxies during the continuous experiments due to

the lack of suitable IR bands sensitive to conformational transitions.

The author wishes to thank Dr. V. Strehmel, University of Halle, for kindly supplying the novolac samples and for many stimulating discussions. Furthermore, I am deeply indebted to Prof. E. Straube, University of Halle, for always giving advice and support.

REFERENCES

1. B. Jasse and J. L. Koenig, *J. Polym. Sci., Polym. Phys. Ed.,* **17,** 799 (1979).
2. H. W. Siesler, *Polym. Bull.,* **9,** 382 (1983).
3. H. W. Siesler, in *Fourier Transform Infrared Characterization of Polymers,* H. Ishida, Ed., Plenum Press, New York, 1987, p. 123.
4. B. Amram, L. Bokobza, J. P. Queslel, and L. Monnerie, *Polymer,* **27,** 877 (1986).
5. Y. Zhao, B. Jasse, and L. Monnerie, *Makromol. Chem., Macromol. Symp.,* **5,** 87 (1986).
6. Y. Zhao, B. Jasse, and L. Monnerie, *Polymer,* **30,** 1643 (1989).
7. P. Chabot, R. E. Prud'homme, and M. Pézolet, *J. Polym. Sci., Polym. Phys. Ed.,* **28,** 1283 (1990).
8. S. Besbes, L. Cermelli, L. Bokobza, L. Monnerie, I. Bahar, B. Erman, and J. Herz, *Macromolecules,* **25,** 1949 (1992).
9. S. Besbes, L. Bokobza, L. Monnerie, I. Bahar, and B. Erman, *Macromolecules,* **28,** 231 (1995).
10. H. S. Lee and S. L. Hsu, *J. Polym. Sci., Polym. Phys. Ed.,* **32,** 2085 (1994).
11. Y. Zhao and H. Lei, *Polymer,* **35,** 1419 (1994).
12. T. Scherzer, *J. Appl. Polym. Sci.,* **58,** 501 (1995).
13. T. Scherzer, *J. Polym. Sci., Polym. Phys. Ed.,* **34,** 459 (1996).
14. T. Scherzer, *Polymer,* **37,** 5807 (1996).
15. H. L. Bos and J. J. H. Nusselder, *Polymer,* **35,** 2793 (1994).
16. J. A. Schroeder, P. A. Madsen, and R. T. Foister, *Polymer,* **28,** 929 (1987).
17. J. A. Schroeder, *J. Mater. Sci.,* **23,** 3073 (1988).
18. P. A. Madsen and R. T. Foister, *J. Appl. Polym. Sci.,* **37,** 1931 (1989).
19. E. B. Stark, A. M. Ibrahim, and J. C. Seferis, *Proceedings of the 28th National SAMPE Symposium,* Anaheim, CA, 1983, p. 581.
20. E. B. Stark, A. M. Ibrahim, and J. C. Seferis, in *Interrelations between Processing, Structure and Properties of Polymeric Materials,* J. C. Seferis and P. S. Theocaris, Eds., Elsevier, Amsterdam, 1984, p. 23.
21. V. Strehmel, B. Strehmel, K.-F. Arndt, G. Müller, and M. Fedtke, *Angew. Makromol. Chem.,* **200,** 125 (1992).
22. V. Strehmel, H. Wetzel, and B. Strehmel, *J. Appl. Polym. Sci.,* **60,** 1221 (1996).
23. H. Dannenberg, *SPE Trans.,* **3,** 78 (1963).
24. V. Strehmel, personal communication.
25. H. W. Siesler, *Makromol. Chem., Macromol. Symp.,* **53,** 89 (1992).
26. H. W. Siesler, *Adv. Polym. Sci.,* **65,** 1 (1984).
27. R. J. Samuels, *Makromol. Chem., Suppl.,* **4,** 241 (1981).
28. H. W. Siesler and K. Holland–Moritz, *Infrared and Raman Spectroscopy of Polymers,* Marcel Dekker, New York, 1980.
29. J. D. LeMay and F. N. Kelley, *Adv. Polym. Sci.,* **78,** 115 (1986).
30. D. Boese, C. D. Eisenbach, E. W. Fischer, H. Hayen, H. Nefzger, G. Planer–Kühne, N. Reynolds, and H. W. Spiess, *Makromol. Chem., Macromol. Symp.,* **50,** 191 (1991).
31. H. Matsuura and K. Fukuhara, *J. Polym. Sci., Polym. Phys. Ed.,* **24,** 1383 (1986).
32. A. S. Argon, *Phil. Mag.,* **28,** 839 (1973).
33. P. B. Bowden and S. Raha, *Phil. Mag.,* **29,** 149 (1974).
34. E. F. Oleinik, *Adv. Polym. Sci.,* **80,** 49 (1986).
35. E. F. Oleinik, *Progress Colloid Polym. Sci.,* **80,** 140 (1989).
36. X. Caux, G. Coulon, and B. Escaig, *Polymer,* **29,** 808 (1988).
37. M. Ochi, N. Tsuyuno, K. Sakaga, Y. Nakanishi, and Y. Murata, *J. Appl. Polym. Sci.,* **56,** 1161 (1995).
38. V. B. Gupta, L. T. Drzal, C. Y.-C. Lee, and M. J. Rich, *Polym. Eng. Sci.,* **25,** 812 (1985).
39. S. Cukierman, J.-L. Halary, and L. Monnerie, *Polym. Eng. Sci.,* **31,** 1476 (1991).
40. M. Ogata, N. Kinjo, and T. Kawata, *J. Appl. Polym. Sci.,* **48,** 583 (1993).
41. R. J. Morgan, C. M. Walkup, F.-M. Kong, and E. T. Mones, *Proceedings of the 30th Natl. SAMPE Symposium,* Anaheim, CA, 1985, p. 391.